Supporting information

Water table fluctuations affect dichloromethane biodegradation in lab-scale aquifers contaminated with organohalides

Maria Prieto[1], Sylvain Weill[1], Benjamin Belfort[1], Emilie E.L. Muller[2], Jérémy Masbou[1], François Lehmann[1], Stéphane Vuilleumier[2], Gwenaël Imfeld[1,*]

[1] Université de Strasbourg, CNRS/EOST, ITES UMR 7063, Institut Terre et Environnement de Strasbourg, Strasbourg, France

[2] Université de Strasbourg, CNRS, GMGM UMR 7156, Génétique Moléculaire, Génomique, Microbiologie, Strasbourg, France

*Corresponding author:

Email address: imfeld@unistra.fr (G. Imfeld)

Manuscript for Water Research

Table of Contents

A. Groundwater sampling

The supplied groundwater was collected from the industrial site of Thermeroil (Varennes-le-Grand, Saône-et-Loire, France; GPS coordinates, 46.701141 N, 4.843919 E). Groundwater was collected from well Pz28 which is located at the source zone of the DNAPL plume (Hermon et al., 2018). Groundwater was stored in three 50 L tanks (Walther Pilot, Wuppertal, Germany) and kept at constant N_2-flux to maintain anoxic conditions. In the laboratory, the 50 L tanks were stored in a temperature-controlled room at 18 ± 1 °C until further analysis.

B. Experimental setup

The two lab-scale aquifers consisted of stainless-steel tanks (dimensions: 160 cm × 80 cm × 7 cm), filled to an average depth of 70 cm with sterilized quartz-sand (grain size: 0.4-0.6 mm). Quartz-sand was sterilized by rinsing with sterile Milli-Q water and dried in an oven at 120 °C for 12h. During the filling procedure, the water table was raised stepwise and maintained above the top of the porous medium to limit the volume of entrapped air. Subsequently, the water table was slowly lowered to its final position (33 cm depth from the bottom) and an unsaturated zone was formed at the upper part of the porous media. A capillary fringe of approx. 12 cm was established visually. Both lab-scale aquifers were continuously fed with contaminated groundwater from a well-characterized industrial site (Hermon et al., 2018). The water table was monitored by tensiometers (ceramic cup and pressure sensors Keller AG, Switzerland) located at 10, 35 and 60 cm depth from the bottom, and at 35, 65, 95, and 125 cm from the inflow. The experiments were carried out in a temperature-controlled room at 18 ± 1 ºC. The inlet and outlet ports were vertically spaced by 5 cm and accounted for 8 ports on each lateral border. Filters (2 mm diameter, porosity 1, DURAN®) were located at each port to avoid sand clogging. Sampling

ports were placed horizontally at 35, 65, 95 and 125 cm from the inflow, and vertically at 15, 40 and 65 cm from the bottom. Samples were taken via stainless steel needles connected to Luer-lock™ stopcocks. A headspace zone of 10 cm above the sand compartments was covered by a top glass mounted with 3 sampling ports equipped with active charcoal cartridges and opened to the atmosphere. Oxygen sensitive optode foils (4 cm × 4cm, PreSens GmbH, Regensburg, Germany) were glued onto the inner side of the front glass pane of the chambers, and measurements were performed using a non-invasive oxygen method (VisiSens, PreSens, GmbH, Regensburg, Germany). Oxygen measurements were corrected by a two-point calibration using air-saturated and oxygen-depleted solutions.

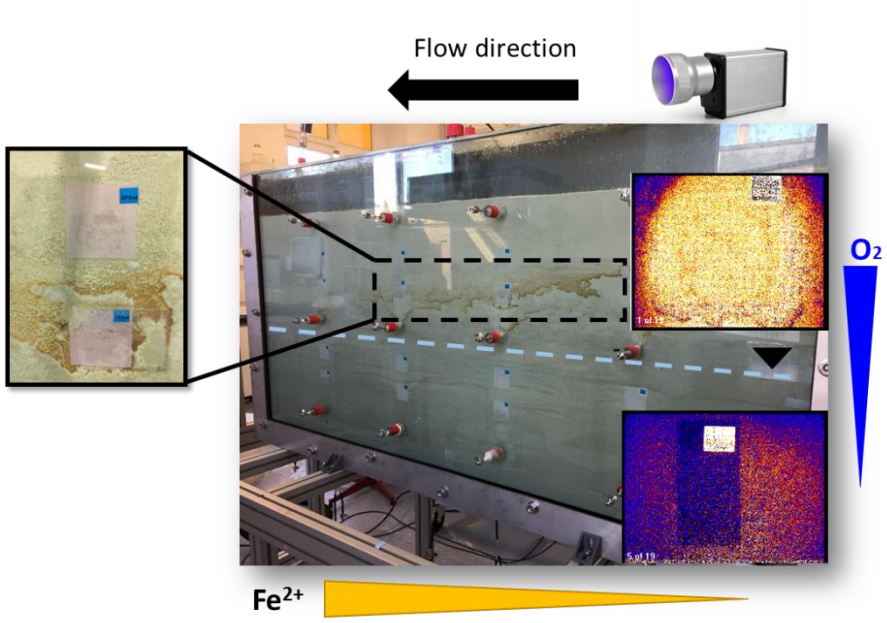

Figure S1. Lab-scale aquifer (at day 88) fed with O_2-depleted spiked-DCM groundwater from a well characterized industrial site. Pictures on the right hand-side of the figure represent snapshots of O_2 foil measurements (4 cm × 4cm, PreSens GmbH, Regensburg, Germany) with a PreSens' modular camera imaging system (VisiSens, PreSens, GmbH, Regensburg, Germany) in the saturated zone and unsaturated zone. In the unsaturated zone, iron precipitates were formed after the incubation period.

C. DCM quantification

For DCM concentration measurements, 200 µL of headspace samples were analyzed in a gas chromatograph (GC, Trace 1300, Thermo Fisher Scientific) coupled with a mass spectrometer (MS, ISQ™, Thermo Fisher Scientific) and equipped with a DB-624 (30 m × 0.32 mm ID, 1.80 µm film thickness) and a flame ionization detector (FID). Helium was used as the carrier gas with a flow rate of 1.5 mL min^{-1}. Sampling was automated using a headspace autosampler (TriPLus RHS™, Thermo Fisher Scientific), and headspace equilibrium was reached by 3 min agitation at 70°C temperature. The GC injector and detector were set at 240 °C and 250 °C, respectively. Headspace samples were injected through a split/splitless injector (split ratio 1:300). The initial oven temperature (35 °C) was held for 3 minutes, then ramped at 10 °C/min to 115 °C followed by an increase to 260 °C at a ramping rate of 30 °C min^{-1}. DCM calibration curves were prepared similarly as the aqueous samples, with the same standard and NaCl ratio (1:1) and headspace volume. Detection limits (DLs) and quantification limits (QLs) were 1 and 64 µg/L, respectively.

D. Compound Specific Isotope Analysis (CSIA) of DCM

Cl-CSIA analysis

Dichloromethane $\delta^{37}Cl$ values were obtained by GC-qMS measurements. A summary of used GC-qMS parameters can be found in Table S1. The chlorine isotope composition of DCM was based on the two most abundant fragment ion peaks $[^{35}Cl^{12}C_1H_2]^+$ (m/z 49) and $[^{37}Cl^{12}C_1H_2]^+$ (m/z 51) (Heckel et al., 2017; Jin et al., 2011). To convert delta values relative to the international reference Standard Mean Ocean Chloride (SMOC), a two-point calibration was performed with two external standards of DCM from Sigma Aldrich ($DCM_{\#1}$) and VWR ($DCM_{\#2}$) suppliers. The external DCM standards ($DCM_{\#1}$ = 3.68 ± 0.10‰ and $DCM_{\#2}$ = -3.35 ±

0.12‰, n=17) were characterized at the Isotope Tracer Technologies Inc., Waterloo, Canada by IRMS after conversion to CH_3Cl (Holt et al., 1997). The two standards were also analyzed at the Departament de Mineralogia, Petrologia i Geologia Aplicada (Barcelona, Spain) by GC-qMS. A shift of $\Delta\delta^{37}Cl = 7.2 \pm 0.6$ ‰ (n=10) was derive between the two standards, validating previous measurements.

These external standards were placed into daily measurement sequences in the following way. At the beginning of a session, six injections of the first standard and six injections of the second standard were performed at different DCM concentrations. This resulted in a series of amplitudes for evaluation of the linearity of the method. Duplicate measurements of both standards were introduced after every ten sample injections to evaluate drift. The measurement sequence was concluded by duplicate measurements of both standards with the same concentration and headspace volumes. All samples were injected 6 times and bracketed with six injections of $DCM_{\#1}$ standard. Typical reproducibility of six injections was 0.5‰ (1σ) within the tested linearity range (0.5 - 20 mg L^{-1}). Values for external standards (after amplitude and drift correction) were plotted against their values on the SMOC scale and sample measurements were evaluated using the intercept and the slope of this regression.

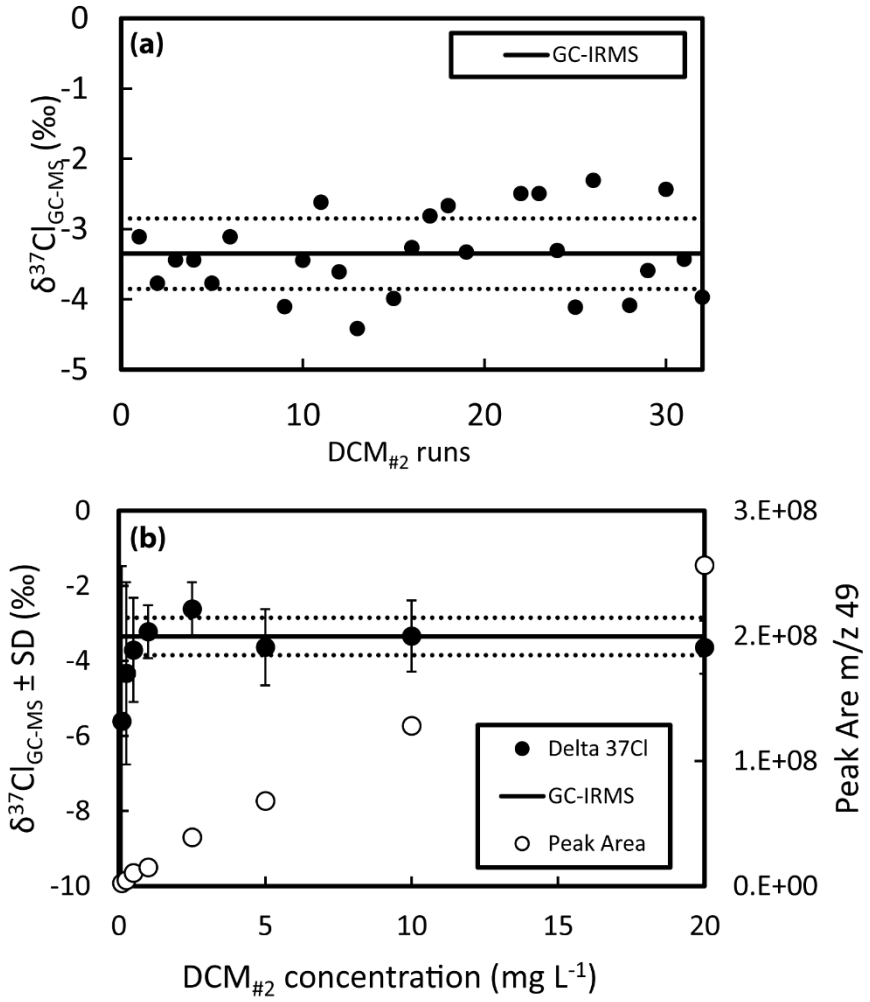

Figure S2. Results of the DCM $\delta^{37}Cl_{GC\text{-}MS}$ validation protocol. (a) Long term reproducibility of $DCM_{\#2}$ standards run over the analytical sessions (concentration range: 1-20 mg L^{-1}). For comparison, $DCM_{\#2}$ $\delta^{37}Cl_{GC\text{-}IRMS}$ consensus mean (black line) associated with typical 0.5‰ uncertainties (dashed lines) have been added to the plot. (b) $DCM_{\#2}$ amount dependence on $\delta^{37}Cl_{GC\text{-}MS}$ measurement within the linearity test. Racketing standard $DCM_{\#1}$ was kept at 10 mg L^{-1} and only $DCM_{\#2}$ concentration varied. For comparison, $DCM_{\#2}$ $\delta^{37}Cl_{GC\text{-}IRMS}$ consensus mean (black line) associated with typical 0.5‰ uncertainties (dashed lines) have been added to the plot.

Table S1. Setup of GC-qMS for chlorine isotope analysis.

Instrument manufacturer	Thermo Fisher Scientific
GC	Trace 1300 (Thermo Fisher Scientific)
qMs	ISQ (Thermo Fisher Scientific)
m/z	49 & 51[a]
EI (eV)	70
Dwell time (msec)	60
Flow (ml min)	1.5
Split	10
Column	DB-624 (30m, 0.32 mm inside diameter, 1.80 µm film thickness, Agilent) Thermo Fisher Scientific
Temperature program	Start at 50°C (2min), 20°C/min to 230°C (0.5 min)
Injection temperature	240 °C
Injection technique	Automated HS
Injection vial	20 mL (18 mL headspace + 2 mL liquid)
Agitator temperature	70
Autosampler	TriPlus RSH (Thermo Fisher Scientific)
Peak integration	Xcalibur™ standard method
Software	Xcalibur™ Software - Thermo Fisher Scientific
Concentration range	0.5 to 20 mg L^{-1}
Calibration slope	1.00 ± 0.02

[a] *Most abundant fragments of DCM.*

C-CSIA Analysis

Stable carbon isotope composition of DCM was determined by gas chromatography - combustion-isotope ratio mass spectrometry (GC-C-IRMS). The GC-C-IRMS system consisted of a gas chromatograph (Trace 1310, ThermoFisher Scientific) coupled via a GC/Conflow IV interface to an isotope ratio mass spectrometer (DeltaV plus, ThermoFisher Scientific). The oxidation furnace of the interface was set to a temperature of 1000 °C. A DB-624 column (60 m × 0.25 mm ID, 1.40 µm film thickness) was used for chromatographic separation at a flow rate of 1.5 mL/min, with helium as the carrier gas. The column was held at 35 °C for 6 min, heated at a rate of 5 °C min^{-1} to 115 °C and held for 7 min, then up to 130 °C at 10 °C min^{-1}, then heated at 20 °C min^{-1} up to 220 °C and held for 2 min. Headspace samples (250 - 500 µL) were injected using a CTC PAL GC autosampler into a split/splitless injector operated in splitless or split mode (7 to 30) at 250°C.

The $\delta^{13}C$ values were calibrated using a three- point calibration of international reference materials AIEA600, USGS40, and USGS41 (σ<0.05‰). Reproducibility of triplicate measurements was ≤0.2‰ (1 σ) within the linearity range of the instrument (5-200 ng of carbon injected on column). A DCM and BTEX standard of known isotopic composition was measured every nine injections for quality control. Carbon isotope ratios were reported in δ notation as parts per thousand [‰] relative to the international reference material Vienna Pee Dee-Belemnite (V-PDB).

E. Oxygen evolution under transient and steady-state conditions

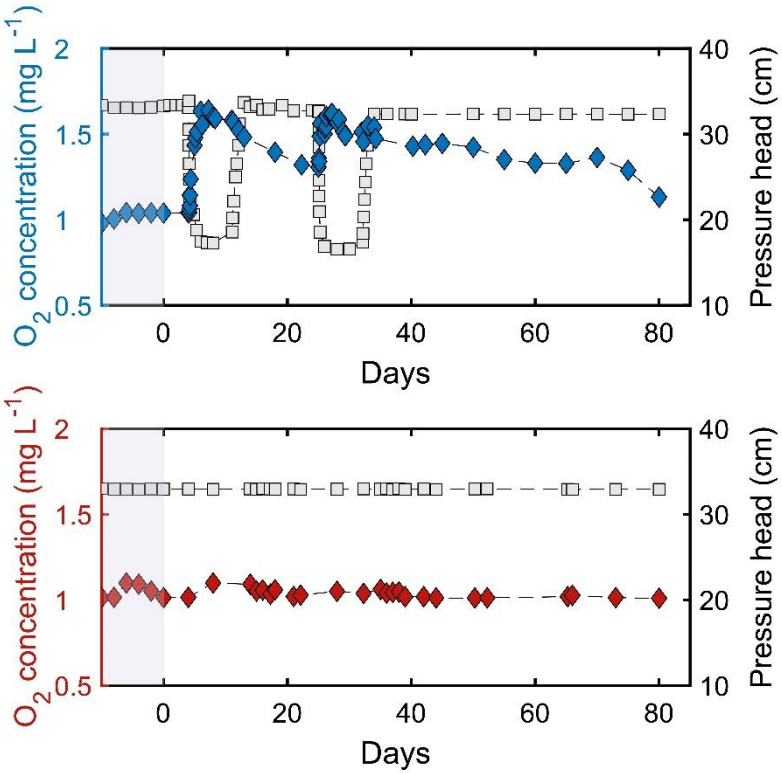

Figure S3. Oxygen concentrations (diamonds) *versus* pressure head (squares) under transient (top blue) and steady-state (bottom red) conditions at depth 25 cm from the bottom. Observation points cover the experimental phase from 0 to 80 days. Grey zones represent the end of the incubation period. Error of measurement: ± 0.4 mg L^{-1}. Inflow groundwater concentrations: 0.7 ± 0.4 mg L^{-1}.

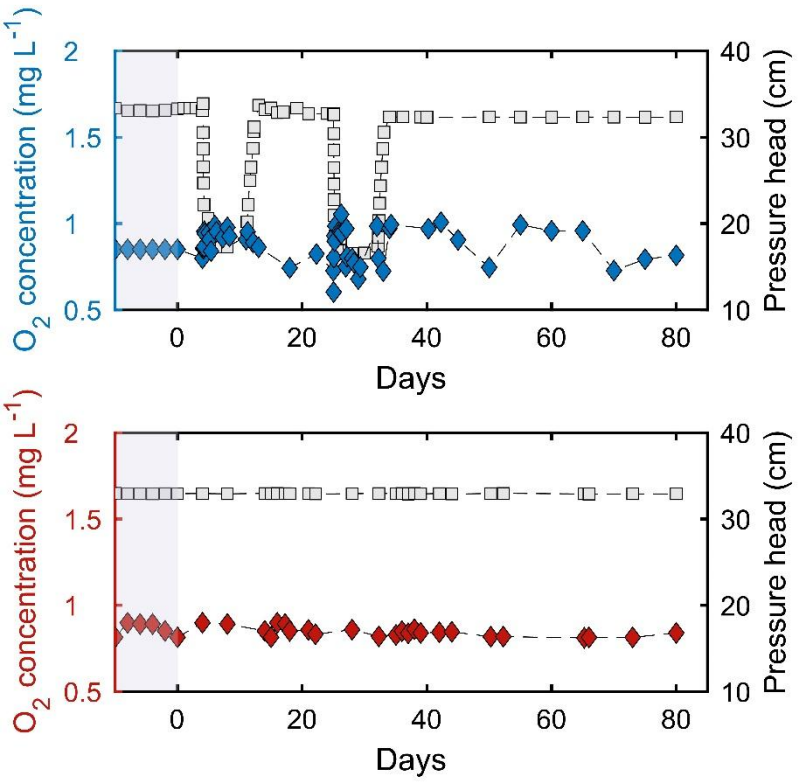

Figure S4. Oxygen concentrations (diamonds) *versus* pressure head (squares) under transient (top blue) and steady-state (bottom red) conditions at depth 10 cm from the bottom. Observation points cover the experimental phase from 0 to 80 days. Grey zones represent the end of the incubation period. Error of measurement: ± 0.4 mg L^{-1}. Inflow groundwater concentrations: 0.7 ± 0.4 mg L^{-1}.

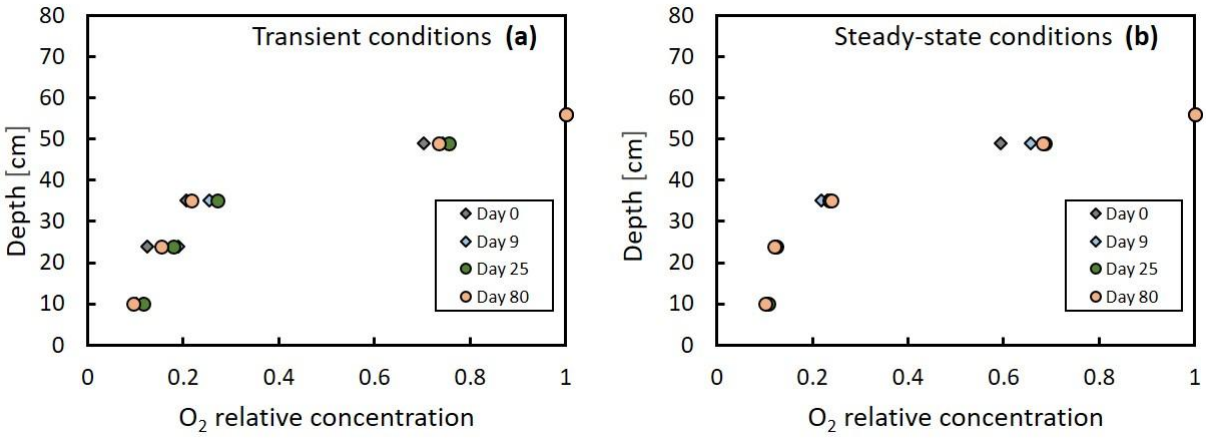

Figure S5. Relative oxygen concentration *versus* depth under transient (a) and steady-state (b) conditions at x = 65 cm from the inflow. Observation points cover the experimental phase from 0 to 80 days. Error of measurement: ± 0.4 mg L^{-1}.

F. Hydrochemistry

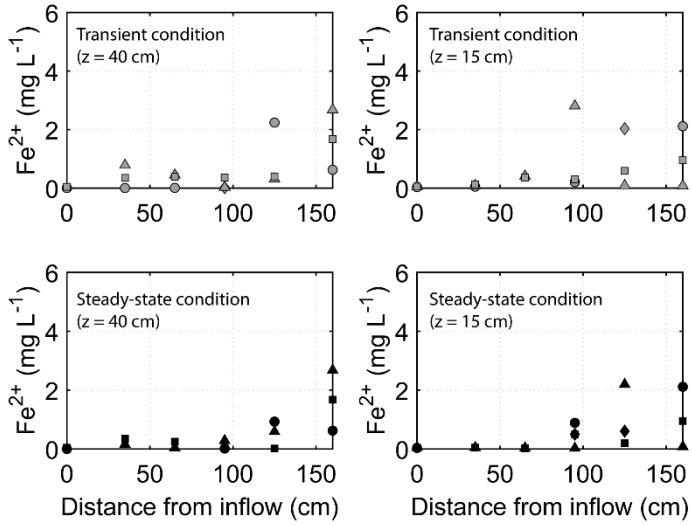

Figure S6. Evolution of Fe(II) concentrations along the flow path in aquifers under steady-state and transient conditions. Symbols represent measured values over distance from the inflow during the investigated period: day 0 (diamonds), day 13 (circles), day 20 (triangles) and day 35 (squares).

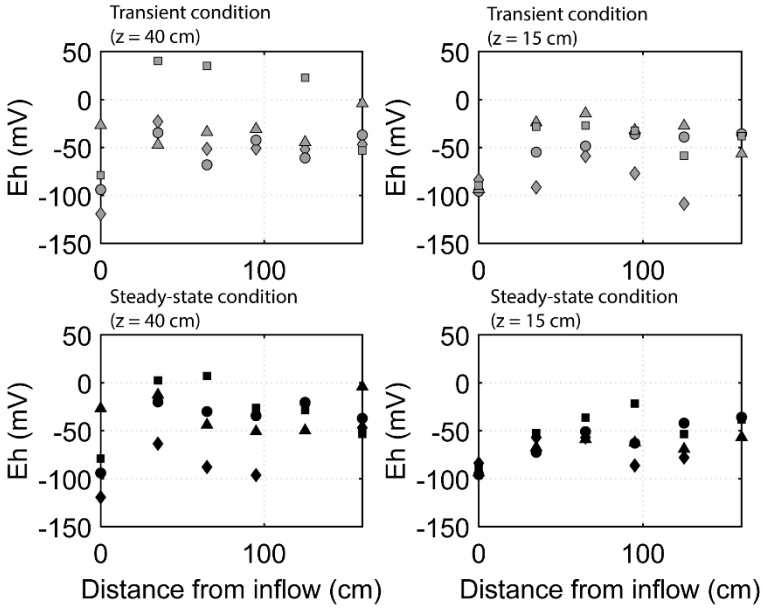

Figure S7. Evolution of Eh along the flow path in aquifers under steady-state and transient conditions. Symbols represent measured values over distance from the inflow during the investigated period: day 0 (diamonds), day 13 (circles), day 20 (triangles) and day 35 (squares).

Table S2. Hydrochemistry of lab-scale aquifers fed with spiked-DCM groundwater under transient and steady-state conditions. Data represent incubation period (inc, n=10), first water table fluctuation (day 0-13, n=20), second water table fluctuation (day 20-35, n=20) and end of the experiment (day 80, n=10). The reported values correspond to mean values of measurements taken at each sampling event from sampling ports located at the inlets, outlets, and depths 15 cm and 40 from the bottom. Reported values for supplied groundwater correspond to the day of sample collection (n=3).

Parameter	**Units**	**Groundwater**	**Aquifer 1: Transient condition (days)**				**Aquifer 2: Steady-state condition (days)**			
			inc[a]	**0-13**	**20-35**	**80**	**inc**	**0-13**	**20-35**	**80**
pH	-	6.7±0.2	6.9[b]±0.1[c]	6.8±0.2	7.1±0.2	6.9±0.2	6.7±0.1	7.0±0.2	7.2±0.1	6.9±0.2
Redox	mV	-170±96	-74±37	-53±27	-8±40	-35±16	-98±28	-55±37	-43±20	-50±25
Elec. Cond.	mS cm^{-1}	2.1±1.0	0.7±0.1	0.8±0.3	1.1±0.3	0.9±0.1	0.7±0.1	0.8±0.1	0.9±0.1	0.9±0.1
Cl^-	mg L^{-1}	450±2	103±30	145±29	135±23	155±36	103±10	130±32	142±64	153±34
NO_3^-	mg L^{-1}	1.9±0.1	< L.Q.	0.5±0.1	0.4±0.1	0.4±0.1	< LQ	0.5±0.1	0.3±0.1	< L.Q.
NO_2^-	mg L^{-1}	< L.Q.[d]	< L.Q.	< L.Q.	< L.Q.	< L.Q.	< L.Q.	< L.Q.	< L.Q.	< L.Q.
Mn^{2+}	mg L^{-1}	161±0.8	37±1.0	34±4.0	28±5.3	33±5.0	37±4.0	34±4.3	29±3.2	35±4.0
Total Fe	mg L^{-1}	-	0.4±0.2	1.4±1.3	0.7±0.8	0.5±0.6	0.6±0.4	1.3±1.2	1.1±1.1	0.5±0.5
Fe^{2+}	mg L^{-1}	14±6	0.5±0.3	0.6±0.8	0.6±0.8	0.5±0.5	0.3±0.2	1.2±0.8	0.6±0.8	0.3±0.3
SO_4^{2-}	mg L^{-1}	68±10	0.9±0.4	0.8±0.3	0.7±0.3	1.1±0.7	1.1±0.5	0.8±0.2	0.5±0.3	0.8±0.1

[a] Total incubation period of 70 days prior to experiments. Data within the incubation period corresponds to sample collection at day 35.
[b] Mean values of n measurements.
[c] Standard deviation (σ) of the mean values of n measurements.
[d] Below limit of quantification

Table S3. Total organic carbon (TOC), non-purgeable organic carbon (NPOC) and inorganic carbon (IC) in lab-scale aquifers fed with spiked-DCM groundwater under transient and steady-state conditions. Data represent incubation period (inc), first water table fluctuation (day 0-13), second water table fluctuation (day 20-35) and end of the experiment (day 80). Values correspond to samples collected from inlet and outlet reservoirs only (n=2).

Parameter	Units	Sample	Aquifer 1: Transient condition				Aquifer 2: Steady-state condition			
			inc[a]	0-13	20-35	80	inc	0-13	20-35	80
TOC	mg L^{-1}	inlet	118[b]±15[c]	110±11	80±13	98±12	76±5	99±6	78±17	90±12
		outlet	106±13	73±30	63±9	52±15	85±6	78±7	73±8	75±7
NPOC	mg L^{-1}	inlet	118±14	120±21	100±6	100±11	100±11	107±6	89±10	96±8
		outlet	106±11	88±16	75±3	61±7	88±5	83±2	84±10	76±5
IC	mg L^{-1}	inlet	56±5	60±7	60±3	50±5	64±3	57±3	65±2	56±4
		outlet	51±5	28±5	23±7	25±6	48±4	41±8	36±5	21±6

[a] Total incubation period of 70 days prior to experiments. Data within the incubation period corresponds to sample collection at day 35.
[b] Mean values of n measurements.
[c] Standard deviation (σ) of the mean values of n measurements.

G. Concentrations and carbon isotope composition of *cis*-DCE and VC

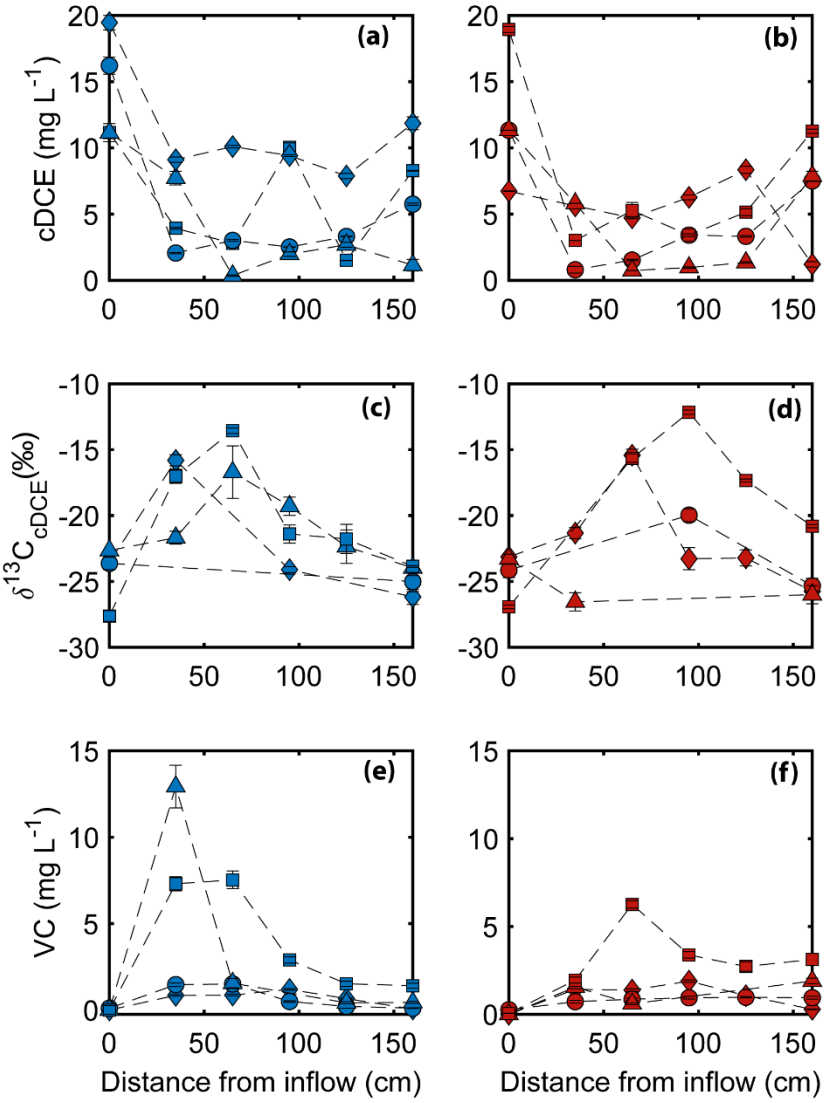

Figure S8. Concentrations and carbon isotope composition of *cis*-DCE and VC under transient (blue) and steady-state (red) conditions. Symbols represent measured values over distance from the inflow during the investigated period: day 0 (diamonds), day 13 (circles), day 20 (triangles) and day 35 (squares). Transformation of *cis*-DCE occurred in both aquifers. The newly formed VC (VC not detected at the inflow) was systematically lighter compared to *cis*-DCE with $\delta^{13}C$ values ranging from −43.56 ± 0.43‰ to −35.7 ± 0.40‰ (n=20).

H. Rayleigh plots of DCM degradation under transient and steady-state conditions

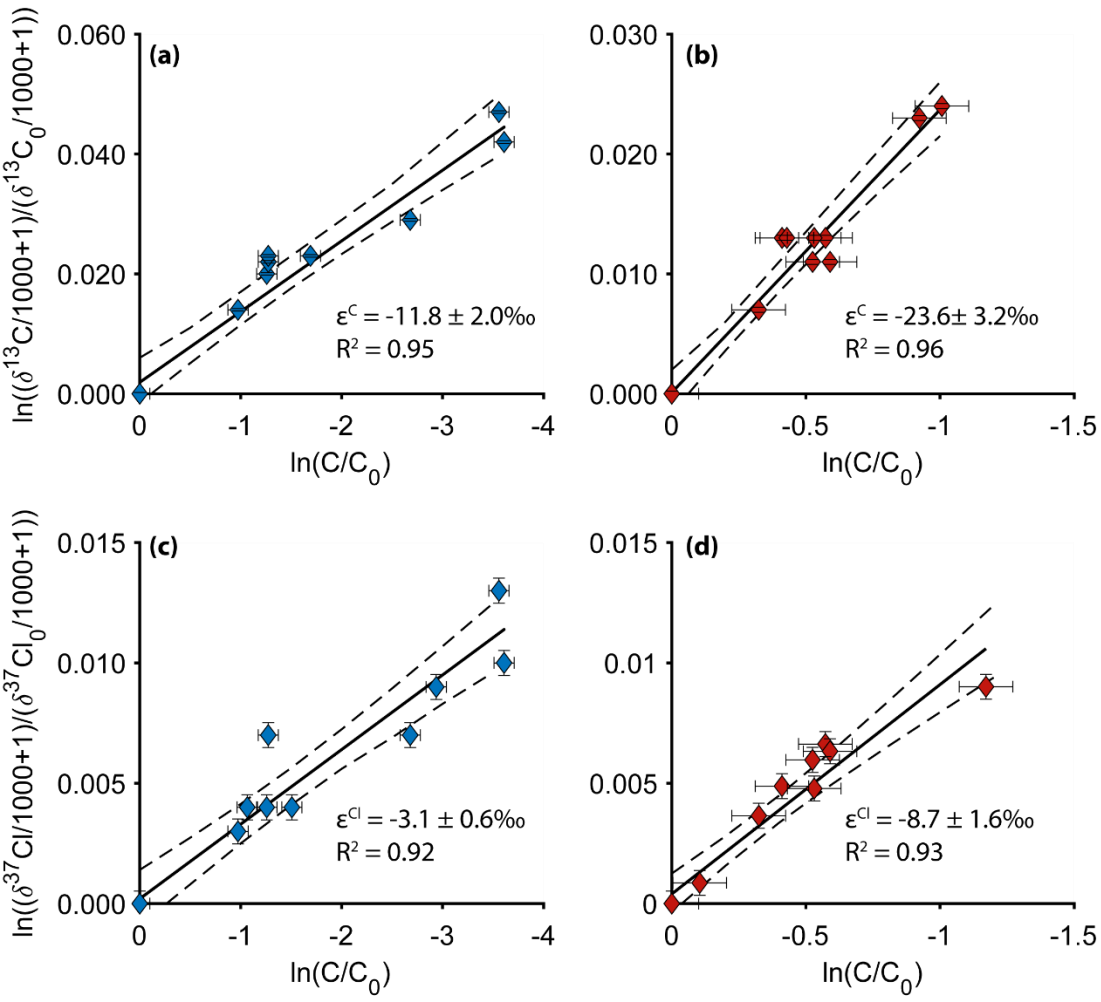

Figure S9. Rayleigh plots of carbon (a, b) and chlorine (c, d) isotope ratios *vs.* residual DCM fraction for DCM degradation in the saturated zone of laboratory aquifers under O_2-depleted conditions from day 0 to 35. Blue: DCM degradation under transient conditions; red: DCM degradation under steady-state conditions. Carbon and chlorine isotope fractionation values (ε^{C}_{bulk} and ε^{Cl}_{bulk}) were obtained from the slope of the linear regression using the Rayleigh model. Error bars represent total uncertainty of isotope ratios. Dashed lines represent the 95% confidence of interval (C.I.).

I. State of the art of proposed DCM degradation pathways based on stable isotopes.

Table S4. Proposed DCM degradation pathways and stoichiometry reactions based on stable isotopes[a].

Experiment	ε^{C} (‰)	ε^{Cl} (‰)	$\Lambda^{C/Cl}$	Degradation pathway	DCM degradation reaction	Source

Aerobic cultures						
Hyphomicrobium sp. strain MC8b	−42.4[b]	−3.8[b]	11.2[b,c]	Glutathione S-transferase	$CH_2Cl_2 + GSH + H_2O \rightarrow CH_2O + 2\,HCl + GSH$	Heraty et al, 1999; Hayoun et al., 2020
Methylobacterium extorquens DM4[d]	−71±2.0	−7.0±0.4	9.5±0.54	Glutathione S-transferase	$CH_2Cl_2 + GSH + H_2O \rightarrow CH_2O + 2HCl + GSH$	Torgonskaya et al, 2019
Anaerobic cultures						
Dehalobacterium formicoaceticum	−42.4±0.7	−5.3±0.1	7.89±0.12	Fermentation harboring WLP	$3CH_2Cl_2 + 4H_2O + CO_2 \rightarrow 2HCOO^- + CH_3COO^- + 9H^+ + 6Cl^-$	Chen et al., 2018, 2020
Mixed culture containing *Dehalobacterium* sp.	−31± 3	−5.2±0.6	5.9±0.3	Fermentation[e]	n.a.	Blázquez-Pallí et al., 2019
Consortium RM harboring *Ca.* Dichloromethanomonas elyunquensis	−18.3±0.2	−5.2±0.1	3.40±0.03	Mineralization (acetogenesis required)[f]	$CH_2Cl_2 + 2H_2O \rightarrow CO_2 + 2H_2 + 2Cl^- + 2H^+$ $4H_2 + 2CO_2 \rightarrow CH_3COO^- + H^+$	Chen et al., 2018, 2020
Ca. Formimonas warabiya strain DCMF	n.a.[g]	n.a.	n.a.	Fermentation harboring WLP	$CH_2Cl_2 + 2H_2O \rightarrow CH_3COO^- + H^+ + 4Cl^-$	Holland et al., 2021
Laboratory aquifers[h]						
Transient conditions	−11.8±2.0	−3.1±0.6	3.58±0.42	Prevailing anaerobic	n.a.	This study
Steady-state conditions	−23.6±3.2	−8.7±1.6	1.92±0.30		n.a.	This study

[a] Uncertainties of ε and Λ values correspond to the 95% confidence interval (CI).
[b] Uncertainties were not provided by the author.
[c] $\Lambda^{C/Cl}$ values were calculated based on reported ε^{C} and ε^{Cl} data by the referenced authors.
[d] *M. extorquens* DM4 cell suspensions: average from "low and high density".
[e] Indication of fermentation pathways with formate and acetate as end products (Trueba-Santiso et al., 2017).
[f] DCM mineralization by *Ca.* D. elyunquensis requires the presence of H_2-consuming partner populations.
[g] n.a.: values were not analyzed/derived.
[h] This study

J. Rarefaction curves for pore water and sand OTUs and bacterial diversity

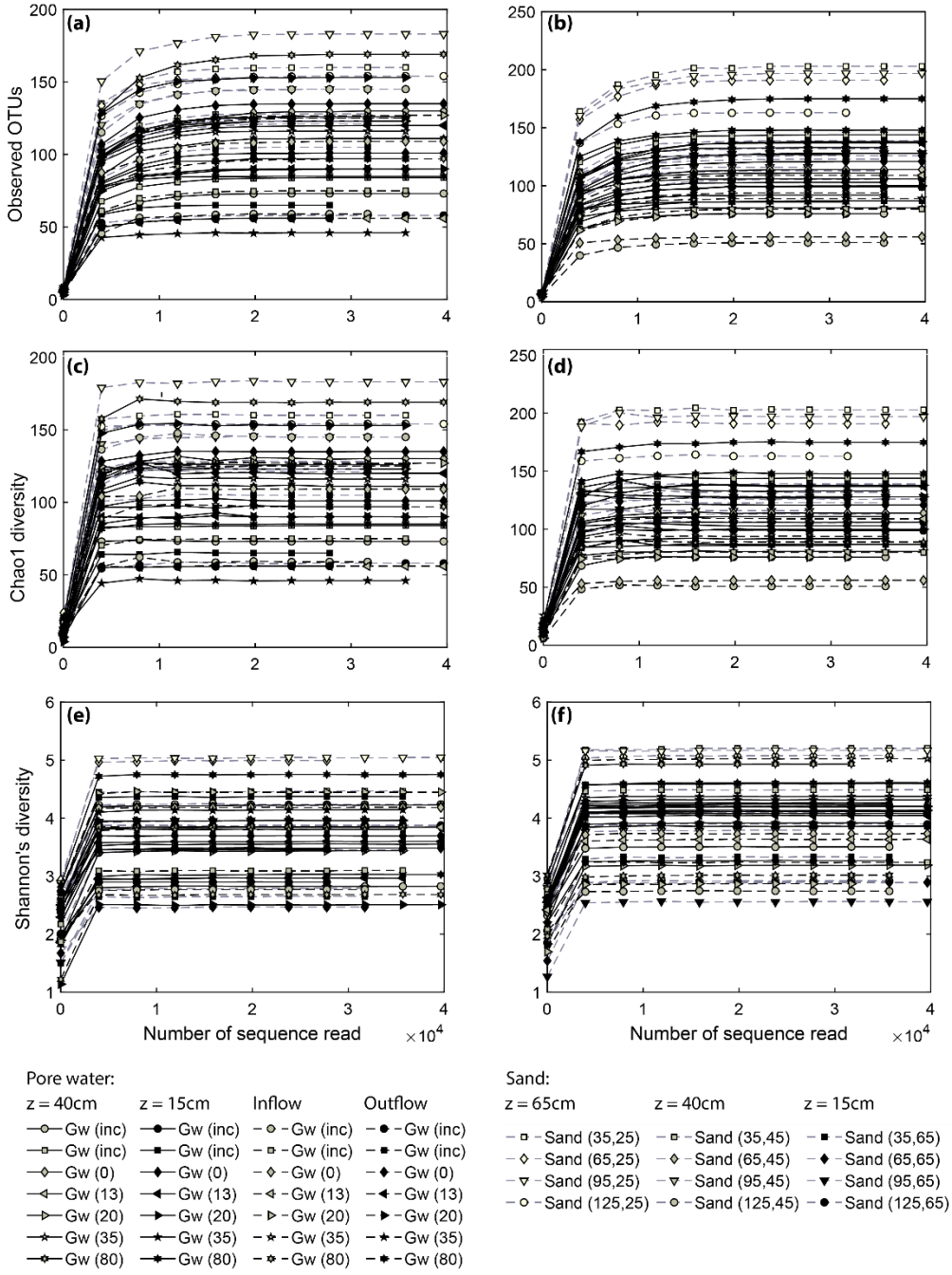

Figure S10. Rarefaction curves based on OTUs (a, b), S_{chaos1} diversity (c, d) and Shannon diversity (e, f) from pore water (Gw) and sand samples under transient (left) and steady-state (right) conditions. Numbers indicated in parenthesis: sand (coordinates x, y) and Gw (in days). Depth is from the bottom of the aquifers.

K. Relative abundance of bacterial communities in pore water samples

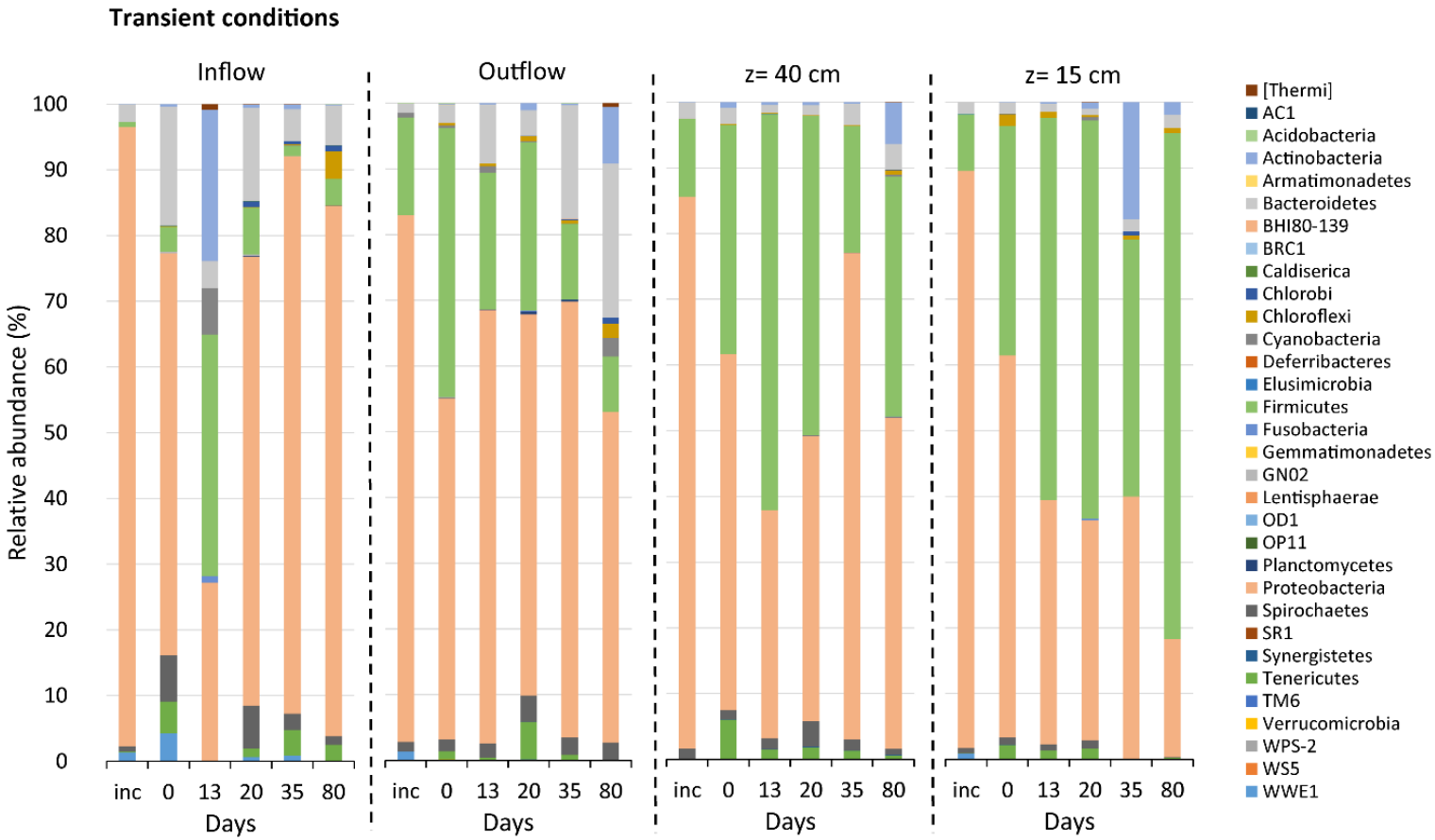

Figure S11. Relative abundance of bacterial phyla in pore water samples over time in DCM contaminated lab-scale aquifer under transient conditions. Sampling event within the incubation period (inc) corresponds to 35 days prior to the experiments.

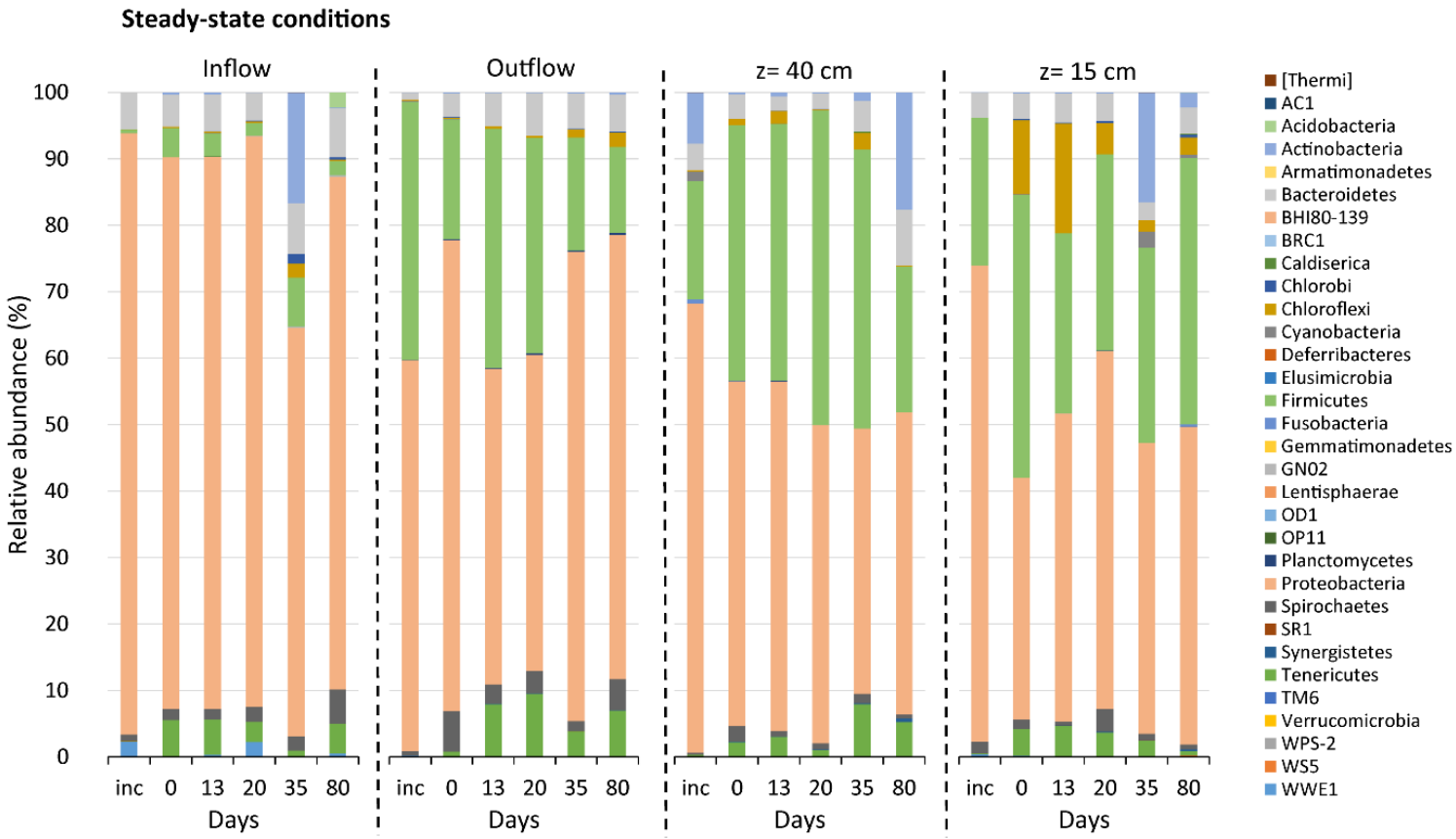

Figure S12. Relative abundance of bacterial phyla in pore water samples over time in contaminated lab-scale aquifer under steady-state conditions. Sampling event within the incubation period (inc) corresponds to 35 days prior to the experiments.

L. Relative abundance of bacterial communities in sand samples

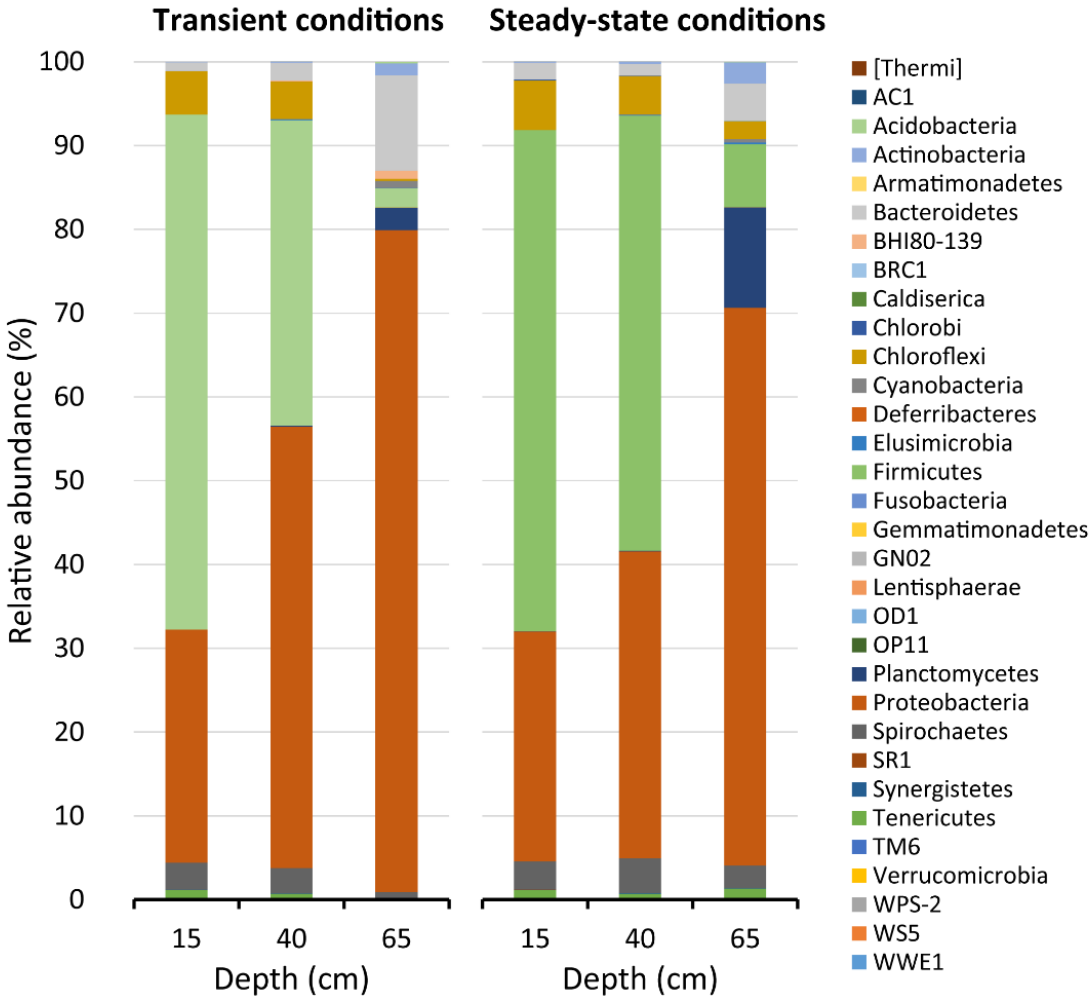

Figure S13. Relative abundance of bacterial phyla in sand samples at day 88 (end of experiment), and at depths of 15, 40 and 65 cm representing anoxic zone, capillary fringe and oxic zone, respectively.

References

1. Blázquez-Pallí, N., Shouakar-Stash, O., Palau, J., Trueba-Santiso, A., Varias, J., Bosch, M., Soler, A., Vicent, T., Marco-Urrea, E., & Rosell, M. (2019). Use of dual element isotope analysis and microcosm studies to determine the origin and potential anaerobic biodegradation of dichloromethane in two multi-contaminated aquifers. Science of The Total Environment, 696, 134066. https://doi.org/10.1016/j.scitotenv.2019.134066

2. Chen, G., Fisch, A. R., Gibson, C. M., Erin Mack, E., Seger, E. S., Campagna, S. R., & Löffler, F. E. (2020). Mineralization versus fermentation: Evidence for two distinct anaerobic bacterial degradation pathways for dichloromethane. The ISME Journal, 14, 959–970. https://doi.org/10.1038/s41396-019-0579-5

3. Chen, G., Shouakar-Stash, O., Phillips, E., Justicia-Leon, S. D., Gilevska, T., Sherwood Lollar, B., Mack, E. E., Seger, E. S., & Löffler, F. E. (2018). Dual carbon–chlorine isotope analysis indicates distinct anaerobic dichloromethane degradation pathways in two members of *Peptococcaceae*. Environmental Science & Technology, 52, 8607–8616. https://doi.org/10.1021/acs.est.8b01583

4. Hayoun, K., Geersens, E., Laczny, C. C., Halder, R., Lázaro Sánchez, C., Manna, A., Bringel, F., Ryckelynck, M., Wilmes, P., Muller, E. E. L., Alpha-Bazin, B., Armengaud, J., & Vuilleumier, S. (2020). Dichloromethane degradation pathway from unsequenced *Hyphomicrobium* sp. MC8b rapidly explored by pan-proteomics. Microorganisms, 8, 1876. https://doi.org/10.3390/microorganisms8121876

5. Heckel, B., Rodríguez-Fernández, D., Torrentó, C., Meyer, A., Palau, J., Domènech, C., Rosell, M., Soler, A., Hunkeler, D., & Elsner, M. (2017). Compound-specific chlorine isotope analysis of tetrachloromethane and trichloromethane by gas chromatography-isotope ratio mass spectrometry vs gas chromatography-quadrupole mass spectrometry: Method development and evaluation of precision and trueness. Analytical Chemistry, 89, 3411–3420. https://doi.org/10.1021/acs.analchem.6b04129

6. Heraty, L. J., Fuller, M. E., Huang, L., Abrajano, T., & Sturchio, N. C. (1999). Isotopic fractionation of carbon and chlorine by microbial degradation of dichloromethane. Organic Geochemistry, 30, 793–799. https://doi.org/10.1016/S0146-6380(99)00062-5
7. Hermon, L., Denonfoux, J., Hellal, J., Joulian, C., Ferreira, S., Vuilleumier, S., & Imfeld, G. (2018). Dichloromethane biodegradation in multi-contaminated groundwater: Insights from biomolecular and compound-specific isotope analyses. Water Research, 142, 217–226. https://doi.org/10.1016/j.watres.2018.05.057
8. Holland, S. I., Ertan, H., Montgomery, K., Manefield, M. J., & Lee, M. (2021). Novel dichloromethane-fermenting bacteria in the *Peptococcaceae* family. The ISME Journal,15, 1709–1721. https://doi.org/10.1038/s41396-020-00881-y
9. Holt, B. D., Sturchio, N. C., Abrajano, T. A., & Heraty, L. J. (1997). Conversion of chlorinated volatile organic compounds to carbon dioxide and methyl chloride for isotopic analysis of carbon and chlorine. Analytical Chemistry, 69, 2727–2733. https://doi.org/10.1021/ac961096b
10. Jin, B., Laskov, C., Rolle, M., & Haderlein, S. B. (2011). Chlorine isotope analysis of organic contaminants using GC–qMS: method optimization and comparison of different evaluation schemes. Environmental Science & Technology, 45, 5279–5286. https://doi.org/10.1021/es200749d
11. Torgonskaya, M. L., Zyakun, A. M., Trotsenko, Y. A., Laurinavichius, K. S., Kümmel, S., Vuilleumier, S., & Richnow, H. H. (2019). Individual stages of bacterial dichloromethane degradation mapped by carbon and chlorine stable isotope analysis. Journal of Environmental Sciences, 78, 147–160. https://doi.org/10.1016/j.jes.2018.09.008
12. Trueba-Santiso, A., Parladé, E., Rosell, M., Lliros, M., Mortan, S. H., Martínez-Alonso, M., Gaju, N., Martín-González, L., Vicent, T., & Marco-Urrea, E. (2017). Molecular and carbon isotopic characterization of an anaerobic stable enrichment culture containing *Dehalobacterium* sp. during dichloromethane fermentation. Science of The Total Environment, 581–582, 640–648. https://doi.org/10.1016/j.scitotenv.2016.12.174